Université de Neuchâtel

Nanotribology at the Solid-Liquid Interface

Thèse

(Version réduite)

présentée à la Faculté des Sciences

pour obtenir le grade de Docteur ès Sciences

par

Martin Binggeli

lic. phil. nat. Université de Berne

Centre Suisse d'Electronique et de Microtechnique (CSEM) S.A.

2007 Neuchâtel

et

Institut de Microtechnique (IMT),

Université de Neuchâtel, 2000 Neuchâtel

Switzerland, 1994

IMPRIMATUR POUR LA THÈSE

Nanotribology at the solid-liquid interface

de M. Martin Binggeli

UNIVERSITÉ DE NEUCHÂTEL

FACULTÉ DES SCIENCES

La Faculté des sciences de l'Université de Neuchâtel sur le rapport des membres du jury,

Messieurs N.F. de Rooij, H.E. Hintermann, R.F. Christoph (CSEM), H. Rohrer (IBM Rüschlikon) et O. Marti (Ulm)

autorise l'impression de la présente thèse.

Neuchâtel, le 7 décembre 1994

Le doyen:

H.-H. Nägeli

List of Publications

- M. Binggeli, R. Christoph, H.E. Hintermann and O. Marti: *Atomic Scale Tribometer for friction studies in controlled atmosphere*, Surface Coatings and Technology **62** (1993) 523.
- M. Binggeli, R. Christoph, H.-E. Hintermann, J. Colchero and O. Marti: *Friction force measurements at potential controlled graphite in electrolytic environment*, Nanotechnology **4** (1993), 59.
- M. Binggeli, G. Kotrotsios, R. Christoph and H.-E. Hintermann: *Novel design for a compact fiber-optic scanning force microscope*, Rev. Sci. Instrum. **64** (1993) 2888.
- M. Binggeli and C.M. Mate: *Influence of capillary condensation of water on nanotribology studied by force microscopy*, Appl. Phys. Lett. **65** (1994) 415.

The complete version of this thesis can be requested at the following address:

Dr. R. Christoph
CSEM
Rue Jaquet-Droz
2007 **Neuchâtel**

Surface and Coatings Technology, 62 (1993) 523–528

Atomic-scale tribometer for friction studies in a controlled atmosphere

M. Binggeli, R. Christoph and H. E. Hintermann
Swiss Center for Electronics and Microtechnology, Inc., Maladière 71, CH-2007 Neuchâtel (Switzerland)

O. Marti
Physics Department, University of Konstanz, D-7750 Konstanz (Germany)

Abstract

To obtain a more fundamental understanding of macroscopic tribological processes, investigations on a microscopic or even atomic scale have to be undertaken. Macroscopic mechanical concepts of adhesion and friction phenomena are not adequate for explaining "nanomechanics". The development of local probe techniques (scanning tunneling microscopy, atomic force microscopy) offered powerful new tools for studying microscopic, *i.e.* local, surface properties. One possible application of these instruments is local friction investigation by simulating a single asperity contact of a real surface with an atomic force microscope tip, and measuring normal and lateral forces occurring at the tip while imaging a sample. With respect to the enormous effect of environmental conditions on which local tribological interactions take place, rigorous control of the atmosphere is needed. We present details of an instrument suited for carrying out local friction investigations in controlled atmospheric conditions or on samples embedded in an extended experimental environment. The instrument's conception and possible applications are described, especially its combination with an electrochemical cell and potentiostatic control of a sample immersed in electrolytes. First results obtained with such a set-up are presented.

1. Introduction

Surface scientists have been investigating tribological phenomena for the last few decades. With a vast variety of methods and concepts, fields such as contact mechanics, fracture kinetics, wear behavior etc. have been investigated with considerable success, as demonstrated by the huge number of publications in the area (see, for example, ref. 1). Although vast, technologically important know-how has been achieved, research activities have always been limited to empirical studies of macroscopic bodies, and no existing theory fully explains the fundamentals of tribological processes. One of the main reasons for this is the lack of knowledge of "nanomechanical" processes, which cannot be derived from classic mechanical approaches [2]. It is generally accepted [3], however, that microscopic, "local" processes have to be considered for the understanding of macroscopic tribological observations.

A possible concept for a real tribosystem under ambient conditions is given in Fig. 1. The integral properties of a large number of single asperity contacts are responsible for the macroscopically manifested friction and wear phenomena. Obviously, the environment in which the asperity interactions take place not only affects the single contacts themselves but, consequently, also the integral macroscopic tribobehavior. Because virtually all solid surfaces under ambient conditions are covered with a water film, there will also be present some solvated ionic species, adsorbates, organic impurities etc. Therefore, knowing the exact state of the local surface properties is crucial to extracting reproducible and interpretable data of investigations on a nanometer scale.

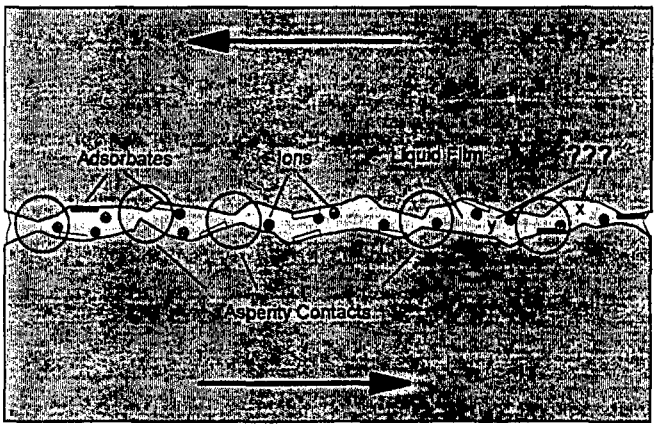

Fig. 1. Possible concept of a real tribosystem under ambient atmospheric conditions. Two touching bodies, moving one relative to the other, share a water film containing solvated ions, adsorbates and other unknown species. The areas of interaction, *i.e.* the single asperity contacts, are shown in circles.

Only recently, powerful tools have been developed which give access to surface properties on a nanometer scale. The introduction of scanning tunneling microscopy (STM) [4] and related scanning probe techniques, such

0257-8972/93/$6.00

as atomic force microscopy (AFM) [5], has opened new ways for locally probing the surfaces of a wide variety of samples and learning more about structural and electronic characteristics of surfaces, from submicrometer down to atomic dimensions. Most interestingly, these techniques can be performed *in situ*, *i.e.* in principle, there is no obstacle to carrying out scanning probe microscopy (SPM) experiments on biological material [6] or on solids immersed in liquids [7, 8].

One important application of these new tools is the simulation of a single asperity contact with an AFM tip [9, 10] (Fig. 2), and the possibility of recording local force interactions between the tip and sample as they move against each other. As mentioned before, rigid control of the environment is essential. Generally, this problem is solved by carrying out the experiments in a UHV chamber. It is also possible to perform surface investigations in a potentiostatic set-up, as known for electrochemical studies of conducting materials.

In a very recent study, the authors showed the potential of combining these two experimental techniques for so-called friction force microscopy (FFM) in an electrochemically controlled environment [11]. This study showed the specific features which a microscope would need for friction studies in a controlled atmosphere.

The aim of the present contribution is to introduce an improved research instrument which permits us to cover this new field of tribological investigations. The instrument will be referred to as an atomic scale tribometer (AST).

2. Instrumental details

Atomic force microscopy is now an established technique for surface investigations—mostly three-dimensional imaging—in the submicrometer range. The principle consists of pulling a sharp tip mounted on a small spring (generally called a cantilever (CL)) over a surface and registering the spring deflections which occur, exactly as in a conventional profilometer, except with much higher resolution. In conventional force microscopy, the sample is mounted on a piezo-tube and scanned relative to the force probe. The resulting output of an appropriate deflection detector can be used to monitor directly changes in the vertical position of the CL induced by height variations of the sample, or to drive a control loop acting on the sample piezo to maintain a constant interaction force between the tip and sample. Originally, bent and etched wires were used as force probes, while nowadays it is usually micromachined silicon and Si_3N_4 levers which come to application.

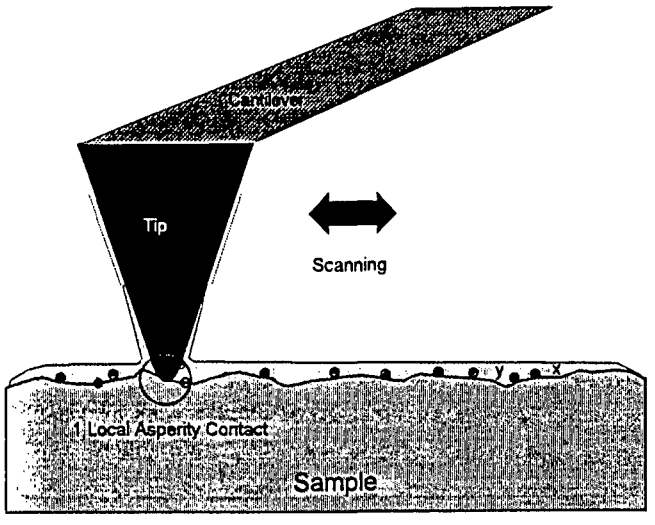

Fig. 2. Same situation as in Fig. 1 but upper surface replaced by an AFM tip to simulate a single asperity contact with local control of the interactions forces.

One possible way to detect very small CL motions is using the so-called beam deflection method [12, 13]. This consists of a laser beam being deflected on the back of the mirror-like CL into a segmented photodiode. The method has two main advantages over other commonly used techniques, such as interferometric [14] or capacitive [15, 16] approaches: it is a long-range detection system, so it is not necessary to have components of the detector in very close proximity to the probe; the two-dimensional character of the method permits simultaneous detection of two orthogonal motions of the CL, one independent of the other, with one single beam and detector.

The second point is the crucial one with respect to atomic-scale tribology, because, by using a four-segmented photo diode, it allows for simultaneous detection of the vertical motions of the CL due to local normal force interaction between the tip and sample and of torsional CL motions due to local lateral force interaction. Of course, this concept is only correct when the scanning direction is perpendicular to the length axis of the CL. The principle was previously proposed by Marti *et al.* [10] and Meyer and Amer [17]. The sensitivity is sufficiently high to obtain atomically resolved images, even from lateral force data (for example, mica [9]), or to detect individual molecules of a Langmuir–Blodgett film [18].

Having the facility of two detectable directions in one detection unit allows for a compact instrument layout. This allows for a so-called stand-alone instrument [19], where the force detector itself is scanned and integrated with the scanning and detection unit into an independent measuring head.

Figure 3 shows a technical drawing of the instrument. The basic concept is to guide a laser beam through a piezotube (x,y,z motion) down onto the CL and back up into the detector. To decouple the beam coming from

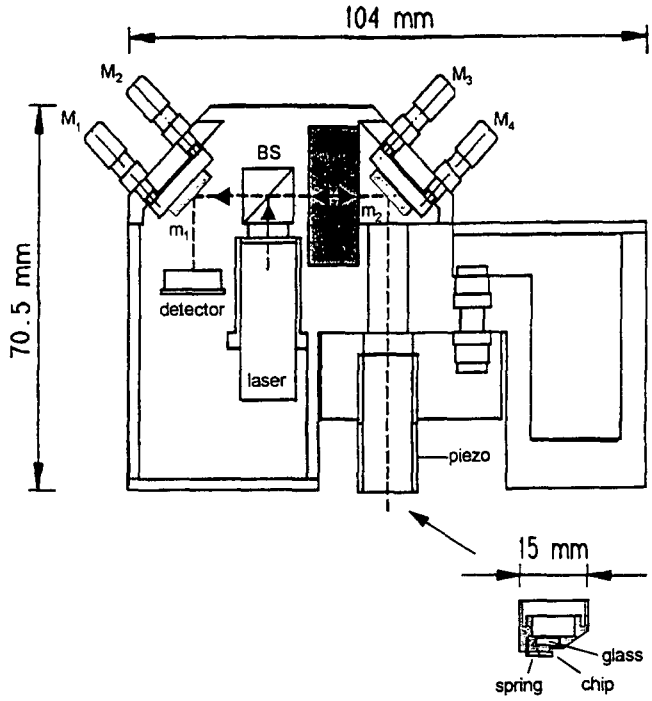

Fig. 3. Schematic drawing of the AST. Visible are the laser diode, the detector diode, the beam splitter cube (BS), the $\lambda/4$ retardation plate, the two mirrors m_1 and m_2, the miniaturized micrometer screws (M_1–M_4) the piezotube and an enlarged view of the piezocap with the cantilever fixation. The laser beam is denoted by a broken line. The small arrows indicate the propagation direction of the light. Not visible is the approach system, including the stepper motor.

the laser diode and the beam reflected from the CL, we use a polarizing beam-splitter cube combined with a $\lambda/4$ retardation plate. In addition to retarding the beam phase, the $\lambda/4$ plate has the effect of turning the polarization plane of the light by an angle of 45°. The cube, correctly installed relative to the $\lambda/4$ plate, causes a deviation of 90° in the beam at its first passing and no deviation at the second passing. Thus, the light is guided into the detector without disturbing the laser with backscattered light.

The major goal of the development was the implementation of the bidirectional force detection system in a device for quantitatively investigating "real" surfaces under "realistic" conditions, which implied a series of technical alterations to the basic concept. A more compact layout was designed, principally for stability reasons, which was aimed at reducing the number and size of the optical components to an absolute minimum. This also has positive effects on the adjustment delicacy of the instrument and improves the signal/noise ratio by lowering the intensity loss caused by each individual component. Two mirrors (m_1 and m_2 in Fig. 2) have been incorporated into the instrument. Together with two miniaturized micrometer screws for each mirror (M_1–M_4), they have to accomplish two functions: first, to compensate for slight deviations of the optical axis to focus the beam onto CL and detector; secondly, to allow easy, reproducible and fast calibration of the instrument in both relevant axis. The mirrors can be moved orthogonally around their height and lateral axes by rotating the corresponding screw. (The calibration procedure is described in Appendix A.) This system is precise and rigid enough to guarantee the reproducibility of the experiments and the time stability of the optical set-up.

The piezotube scanner is mounted on a ground plate and exchanged. On the piezo's end, a cap of insulating material (Nitralon®) is fixed (see Fig. 3), which serves as a CL holder as well as piezo protector when working in liquids. The CL holder geometry permits us to see the lever from outside the microscope with a monocular, which is necessary for beam focusing and for optical approach control.

To achieve a real stand-alone system which may work under particular conditions (see next section), the instrument has been equipped with a stepper motor, acting on a screw located in the back of the microscope, which allows for a step size during the approach of about 20 nm. The instrument was made fully compatible with commercial data acquisition and image process electronics and software (Park Scientific Instruments, Sunnyvale, CA) by means of an interface box. This allowed monitoring of the lateral force data using a free AD/DA converter. Furthermore, the interface houses a preamplifier for the four-segment photodiode and an option for reading out electrochemical data (see below).

3. Modes of operation

The stand-alone principle of the AST is ideally suited for carrying out friction studies under controlled atmospheres. Unlike in conventional AFM, a stand-alone system does not imply any principal limitation to sample dimensions or to the environmental conditions in which the investigations take place. The authors mainly see the following fields of application for this type of instrument:

(1) the investigation of large or heavy samples can be directly achieved by placing the microscope directly on top of the sample;

(2) delicate samples (such as wafers) may also be investigated by turning the microscope around and placing the sample on top of it;

(3) *in situ* investigation can be made of surface properties under controlled environmental conditions, for example, in a closed box without the possibility of manually operating the instrument, like a nitrogen chamber or a calorimeter.

(4) the operation in combination with an electrochemical cell, as described in the next section.

4. Friction investigations in a controlled liquid–solid interphase

As described in the Introduction, local tribological properties are very much affected by the state of the surface being investigated. Our approach involves combining the AST with a standard electrochemical environment for SPM (described before in refs. 20–23, for example), *i.e.* a three-electrode potentiostatic control, with the sample acting as the working electrode in combination with separate reference and counter-electrodes. The cell design and potentiostatic set-up are schematically depicted in Fig. 4. The cell consists of three compartments, separated from each other by ZrO_2 diaphragms.

In principle, the AST may be combined with a wide variety of electrolytic cell designs. In the present system, however, we chose a design which fits directly into the base unit of the previously mentioned commercial system.

5. Results

Figure 5 shows an example of a friction experiment carried out under controlled atmosphere; normal force (corresponding to the topography) (Fig. 5(a)) and lateral force images (Fig. 5(b)) were measured simultaneously, the highly oriented pyrolytic graphite (HOPG) sample being immersed in 0.1 M $NaClO_4$ electrolyte during the imaging process. The potential was measured *vs.* a Pt/H_2 reference system.

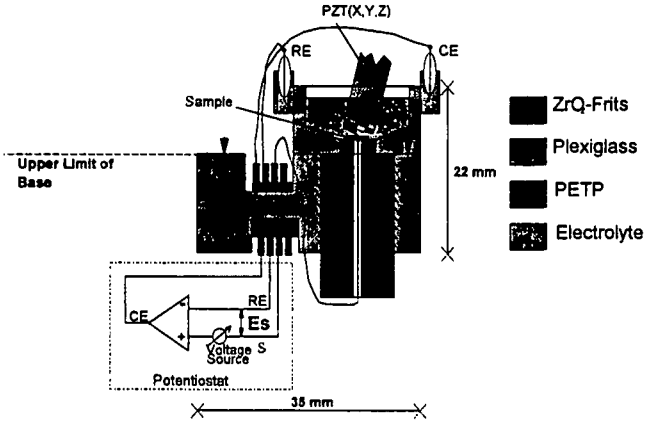

Fig. 4. Schematic representation of the electrochemical cell for carrying out *in situ* friction force experiments with potential control of the sample. The principle of the potentiostatic set-up is also depicted. RE and CE stand for reference electrode and counterelectrode, respectively, and E_S is the potential difference between the sample and reference, *i.e.* "the sample potential". RE and CE cell compartments are separated from the main (working electrode) compartment by ZrO_2-diaphragms. PZT labels the scanning unit of the AST, which is placed above the cell as indicated.

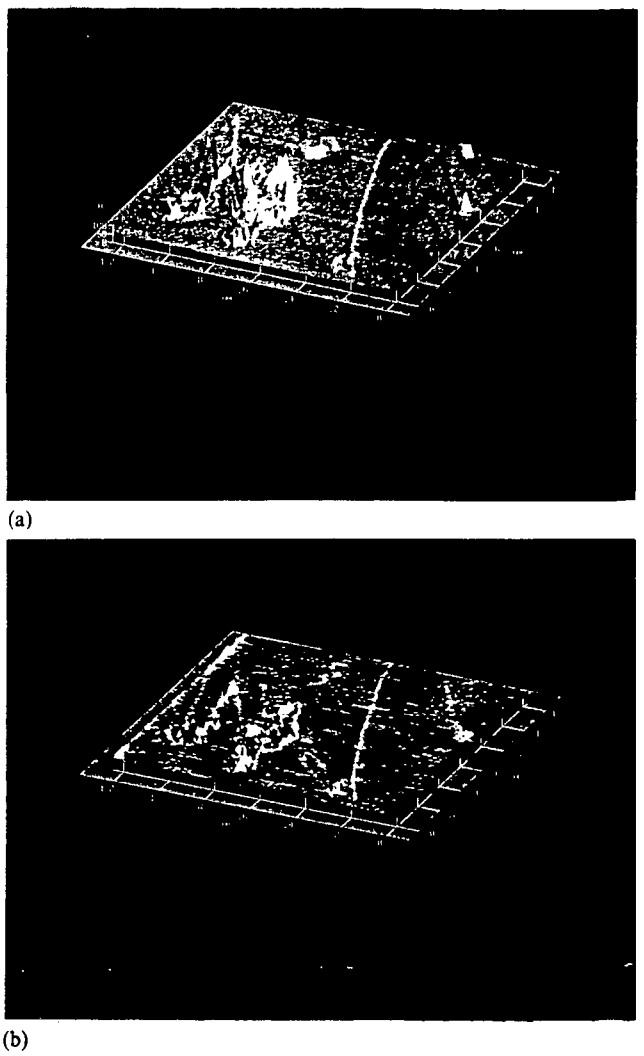

(a)

(b)

Fig. 5. Three-dimensional representation of AFM–FFM measurement of an area 1.25 μm × 1.25 μm of an HOPG sample immersed in 0.1 M $NaClO_4$, recorded at a constant sample potential (−200 mV *vs.* Pt/H_2), and showing (a) the topographic and (b) the lateral force data (force variation black/white about 35 nN). The correlation between topographic features and lateral force variation is clearly visible. The deviation of the force variation always has the same sign.

The general findings are that delicate samples may be imaged in a less destructive way, and that chemical interactions between the tip and sample, manifesting in the lateral force interaction, may be detected. The steps and bumpy features visible in the topographic image (Fig. 5(a)) induce alterations of the lateral force (Fig. 5(b)), which shows an otherwise constant behavior. This observation is consistent with the expectations for a chemically homogeneous surface, where no lateral force variations should occur, except those due to geometric effects. The fact that the variations always have the same direction (higher force values), independent of the step slope, excludes a purely geometric phenomenon. A possible interpretation is that chemical interactions between tip and step edges (*e.g.* dangling bonds, adsorbates) lead to

the observed increase in the lateral forces. Nevertheless, the effects need to be studied more systematically before giving a more stringent interpretation of the results. However, the capability of FFM to detect variations in the chemical characteristics of the sample surface has also been observed by other groups [17, 25], and has been labeled "chemical sensitivity".

6. Conclusions and outlook

It has been shown that local friction forces, as measured with the AST, depend strongly on the chemical composition and environment of the sample under investigation. Therefore, we would like to point out the previously mentioned "chemical sensitivity" of the instrument presented in this contribution. It shows great potential for *in-situ* surface investigations in such fields as biology and electrochemistry. The study of the nanometer-scale friction behavior of potential-controlled samples in the presence of aqueous electrolytes opens new perspectives to a more fundamental understanding of tribological phenomena occurring under realistic environmental conditions.

The stand-alone principle of the AST permits us to investigate the surfaces of sample of practically unlimited size or of samples embedded in an environment of important dimensions. This feature opens a new range of applications in many technical fields, since the sample no longer has to be brought to the instrument and is not limited by the dimensions of the sample holder or scanning unit, as in conventional AFM applications. Moreover, the AST can be regarded as a member of a new class of instruments which can be run on site, wherever specific surface analytical information is required.

Acknowledgments

The authors would like to thank S. Droz, P.-A. Feuz and J.-P. Jeanneret for competent technical assistance, J. Colchero for generous cooperation, and R. Constantin and J. Burger for many helpful discussions.

References

1 D. Dowson, *History of Tribology*, Longman, London, 1979.
2 U. Dürig and O. Züger, *Proc. NATO-ARW on Manipulation of Atoms under High Fields, Lyon, France, 1992*, Kluwer, Dordrecht, p. 271.
3 G. M. McClelland and S. R. Cohen, in R. Vanselow and A. Howe (eds.), *Chemistry and Physics of Solid Surfaces VIII, Springer Ser. Surf. Sci., 22* (1990) 419 and references cited therein.
4 G. Binnig, H. Rohrer, Ch. Gerber and E. Weibel, *Phys. Rev. Lett., 50* (1983) 120.
5 G. Binnig, C. F. Quate and Ch. Gerber, *Phys. Rev. Lett., 56* (1986) 930.
6 G. Binnig, *Proc. 6th Int. Conf. on STM, Interlaken, Switzerland, 1991, Ultramicroscopy, 42–44* (1992) 7.
7 R. Sonnenfeld and P. K. Hansma, *Science, 232* (1986) 221.
8 O. Marti, B. Drake and P. K. Hansma, *Appl. Phys. Lett., 51* (1987) 484.
9 C. M. Mate, G. M. McClelland, R. Erlandsson and S. Chiang, *Phys. Rev. Lett., 59* (1987) 1942.
10 O. Marti, J. Colchero and J. Mlynek, *Nanotechnology, 1* (1990) 141.
11 M. Binggeli, R. Christoph, H.-E. Hintermann, J. Colchero and O. Marti, Friction force measurements at potential controlled graphite in electrolyte environment, *Nanotechnology, 4* (1993) 59.
12 N. M. Amer and G. Meyer, *Bull. Am. Phys. Soc., 33* (1988) 319.
13 S. Alexander, L. Hellemans, O. Marti, J. Schneir, V. Elings and P. K. Hansma, *J. Appl. Phys., 65* (1989) 164.
14 D. Rugar, H. J. Mamin, R. Erlandsson, J. E. Stern and B. D. Terris, *Rev. Sci. Instrum., 59* (1988) 2337.
15 G. Neubauer, S. R. Cohen, G. M. McClelland, D. Horne and C. M. Mate, *Rev. Sci. Instrum., 61* (1990) 2296.
16 J. Brugger, N. F. de Rooij, M. Binggeli, Ph. Renaud and R. Christoph, Capacitive AFM microlever with combined sensor/actuator functions, *Proc. 7th Int. Conf. on Solid State Sensors and Actuators, Yokohama, 1993*, in press.
17 G. Meyer and N. M. Amer, *Appl. Phys. Lett., 56* (1990) 2100.
18 R. M. Overney, E. Meyer, J. Frommer, D. Brodbeck, R. Lüthi, L. Howald, H.-J. Güntherodt, M. Fujihira, H. Takano and Y. Gotoh, *Nature, 359* (1992) 133.
19 M. Hipp, H. Bielefeldt, J. Colchero, O. Marti and J. Mlynek, *Proc. 6th Int. Conf. on STM, Interlaken, 1991, Ultramicroscopy, 42–44* (1992) 1498.
20 P. Lustenberger, H. Rohrer, R. Christoph and H. Siegenthaler, *J. Electroanal. Chem., 243* (1988) 225.
21 O. Lev, F.-R. Fan and A. J. Bard, *J. Electrochem. Soc., 135* (1988) 783.
22 M. Binggeli, D. Carnal, R. Nyffenegger, H. Siegenthaler, R. Christoph and H. Rohrer, *J. Vac. Sci. Technol. B, 9*(4) (1991) 1985.
23 H. Siegenthaler, in H.-J. Güntherodt, R. Wiesendanger (eds.), *Scanning Tunneling Microscopy, Springer Series in Surface Science, Vol. 28*, Springer, 1992, and references cited therein.
24 J. Colchero, H. Bielefeldt, A. Ryf, M. Hipp, O. Marti and J. Mlynek, *Phys. Status Solidi A, 131* (1992) 73.

Appendix A: Force calibration procedure

A rotation of one of the micrometer screws M_1–M_4 (Fig. 3) causes a well-defined beam translation on the photodiode, vertically or laterally, correlated with an also well-defined output signal of the electronics. Knowing the geometry of the instrument and the relevant force constants of the lever, one has the possibility of direct access to the absolute forces acting on the tip. The absolute deviation angles of the CL in both directions (which are then converted into force values) can be found as follows.

The absolute angle of deviation is given by

$$\Delta\phi_i = \frac{\Delta_i}{L_i} \tag{A1}$$

where ϕ_i is the normal or lateral deviation of the lever,

Δ_i is the known deviation on the previously calibrated photodiode and L_i is the absolute distance between the lever and photodiode.

Together with the relationship between spot location and photovoltage (sensitivity of the diode), as given by $\varepsilon = \Delta U/\Delta\phi$, we obtain a calibration factor $e_{\phi i}$ for normal and lateral displacements as follows:

$$e_{\phi i} = \frac{1}{\varepsilon} = \frac{\Delta\phi_i}{\Delta U_i} = \frac{\Delta_i}{\Delta U_i L_i} \tag{A2}$$

For a given geometry, the only unknown factor is Δ_i, which is calibrated before with mirror m_1, *i.e.* screws M_1 and M_2. The calibration has to be redone for each experiment, because of variations of the lever geometry and no infinite time stability of the mechanical and electronic devices. Although the calibration factor $e_{\phi i}$ is not equal for both directions, because of the difference in ε (owing to the asymmetry of the laser spot), eqn. (A2) remains unchanged.

For calculating absolute lateral force values, one has also to take into account the height of the tip (generally about 5 μm).

Nanotechnology 4 (1993) 59–63. Printed in the UK

Friction force measurements on potential controlled graphite in an electrolytic environment

M Binggeli†, R Christoph†, H-E Hintermann†, J Colchero‡ and O Marti‡

†Centre Suisse d'Electronique et de Microtechnique, CH-2007 Neuchâtel, Switzerland
‡Fakultät für Physik, Universität Konstanz, D-7750, Konstanz, Germany

Received 9 September 1992, accepted for publication 29 January 1993

Abstract. We show the simultaneous recording of normal and lateral forces arising in scanning force and friction microscopy on a potential controlled sample immersed in aqueous electrolyte. As a liquid film is present on virtually all solid surfaces under ambient conditions, it is important to control the properties of the solid/liquid interface. In order to obtain reliable information on the friction behaviour of such a surface, a set-up for potentiostatic control of the sample was established. Experiments have been carried out with a stand-alone scanning force and friction microscope (SFFM), combined with an electrochemical cell providing potential control of the sample. First results of simultaneous normal and friction force measurements, obtained on highly oriented pyrolytic graphite (HOPG) immersed in $NaClO_4$, demonstrate the promising potential of the method.

1. Introduction

The understanding of tribological phenomena has been one of the most extensively treated topics of the last few decades [1]. Nevertheless, this particular topic of surface physics/chemistry, until very recent times, has been exclusively devoted to studies concerning macroscopic bodies (due to technological relevance) and is still in a rather empirical stage. This fact is associated with the relative deficit in the knowledge of microscopic (atomistic) tribological behaviour, caused by the lack of appropriate methods providing information on such a scale.

The introduction of STM [2] and related techniques, foremost SFM [3] and the recent development of scanning force and friction microscopy (SFFM) [4–6], opened new ways to locally probe surfaces of a wide variety of samples (including conductors, non-conductors and biological specimens) and to extract more detailed information about structural, electronical and tribological characteristics of surfaces on nanometer or even atomic dimensions.

As virtually any solid surface under ambient conditions (thus also many tribosystems) is covered with a water layer containing all sorts of contaminants, it is important to control the properties of the solid/liquid interface to get quantitatively interpretable results on e.g. friction forces. There are basically two techniques for rigorously controlling a surface state: firstly, investigating a sample in a UHV chamber, which is very demanding from the experimental point of view, and results obtained this way are far from being easy to translate to real conditions; and secondly, investigating a sample surface covered with aqueous electrolyte under appropriate potential control within an electrochemical cell. Such a set-up allows control of surface properties such as surface tension and ion coverage. We believe that these properties are of considerable relevance for the nanotribological characteristics of surfaces under ambient conditions.

One of the most striking features of the new local probe techniques is their ability to investigate samples immersed in liquids [7, 8]. Therefore the intention was to set up an SFFM experiment, which permits simultaneous *in situ* recording of normal forces as well as lateral forces, plus controlling the sample potential while probing it. Different set-ups for potentiostatic control in scanning probe microscopy (SPM) have been described before [9, 10] and this has proven to be a powerful tool for the *in situ* investigation of many surface processes [11–13].

The aim of the present study is thus to show the feasibility of such an approach towards a better understanding of tribological mechanisms on a nanoscale dimension.

2. Experimental details

2.1. Set-up

In order to perform accurate electrochemical experiments in terms of time stability and contaminant concen-

0957-4484/93/020059+05$07.50

tration, it is imperative to have a non-negligible cell volume. However, such a cell cannot conveniently be implemented on the scanner of a conventional SFM because of inertia restrictions.

Therefore a technique where the probe itself may be scanned (as is usually done in STM), which allows for functional cell layout, is of general interest for the growing field of electrochemical SFM applications. An instrument which is perfectly suited for these kinds of studies is the stand-alone SFFM of Hipp *et al* [14]. It permits one to scan the cantilever over the resting sample and to simultaneously measure normal and lateral forces, using the principle of optical beam deflection onto a four-quadrant photodiode [5, 6]. On a mesoscopic scale, lateral forces acting on the SFM tip are associated with friction [15].

The experiments were performed using a slightly modified version of the SFFM, providing the possibility of a direct calibration of normal and lateral forces [15], which gives access to a quantitative interpretation of the experimental data. The scan area of the instrument is about $7 \times 7\,\mu m^2$ and the z range about $2\,\mu m$.

The microscope was combined with an electrochemical cell providing electrodes for potentiostatic control of the sample (see figure 1). The particular design, including a connector, allows the cell to be plugged directly into the piezo-well of a commercial SFM base [16]. The cell volume is about $1500\,\mu l$.

The sample is set on top of a PETP (polyethyleneterephthalate) cylinder, which can be screwed into the cell from underneath and then be contacted with the implemented connector.

Cell potentials are controlled via adapter electronics with a recently developed potentiostat [17] for SPM applications. Data acquisition and processing were performed with PSI electronics and software [16]. The lateral force signal was pre-amplified and then recorded with an additional ADC input of the electronics.

In order to protect the scanning piezo from electrolyte it was covered with an insulating varnish.

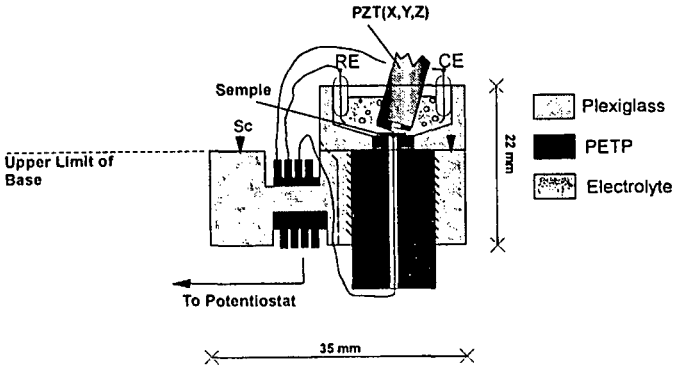

Figure 1. Specially designed electrochemical cell for fitting into the piezo-well of the PSI SPM [16]. The two arrows (one of them labeled 'Sc') show where it can be screwed to the base. RE and CE stand for reference and counter electrode respectively. Of the stand-alone SFFM, only the piezo-tube shown. The microscope layout can be seen in [15].

2.2. Friction measurements on potential controlled graphite substrates

As a model system, HOPG (highly oriented pyrolytic graphite) [18] immersed in 0.1 M $NaClO_4$ [19] was chosen. The sample, a single crystal of about 5 mm diameter and 1 mm thickness, was contacted with a fine wire and then glued on top of the PETP sample holder with epoxy resin. The sample was cleaved immediately before the experiment, then the cell was filled with electrolyte.

Platinum wires, preconditioned and native respectively, were used as reference and counter electrode (reference system Pt/H_2).

Initial friction experiments were carried out in the ideally polarizable region of the HOPG sample.

3. Results

The left part of figure 2 shows a conventional SFM measurement of a freshly cleaved graphite sample. This particular area was chosen due to its variety of topographic features. Various steps (one to three layers high) are clearly resolved. The right hand side of figure 2 shows a simultaneously recorded unfiltered friction force image. Although disturbed by mains interference ripple, the topographic corrugation is clearly reproduced. Interestingly, the direction of friction force variation is independent, whether the tip passes a step edge downwards or upwards.

This effect can be evidenced by measuring the mean step heights of some consecutive sections through the image along the scan lines. Figure 3 shows a representative example of such a cut, illustrating a comparison of a section through the two steps located in the lower left corner of figure 2; first the topographic (upper trace) then the friction data are depicted.

A statistical analysis of ten consecutive sections yields for the force variation 16.5 ± 2.5 nN for the downward case and 35 ± 3.5 nN for the upward case. These observations can be understood as the sum of two effects: first we have a topographic effect where the lateral force changes sign with the sign change of the slope [15]; second, the tip–sample interaction is different at the steps compared to the flat surface. This phenomenon is associated with a change in the chemical characteristics of the tip–sample interface, for example, dangling bonds from carbon atoms at the step edges, which might attract the tip much more than the continuous surface. A force of equal direction, but different magnitude, as the force caused by the topographic effect sliding up a step, is then required to detach the tip from the edge. The direction of the force is independent of the step slope.

Therefore we conclude that of the total lateral force variation of ~35 nN, 10 nN is due to the topographic effect and 25 nN due to the binding of the tip to the step edge.

At the two small structures marked with an arrow on figure 2, one may see a clear difference in the friction

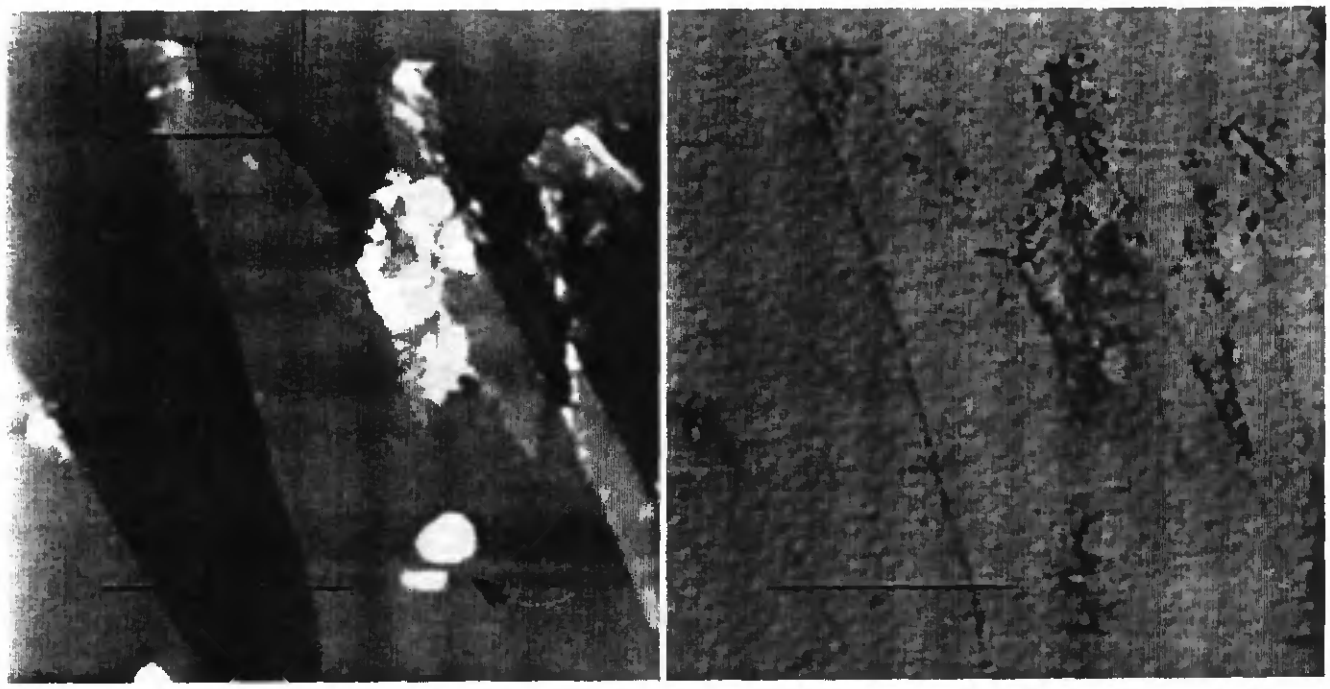

Figure 2. The left part shows a topographic image, the right part a friction force image of a $1.25 \times 1.25\ \mu m$ area of an HOPG sample immersed in 0.1 M $NaClO_4$. The sample potential was -200 mV versus NHE. The height variation is from 0 Å (black) to 80 Å (white), the lateral force variation from 40 nN (black) to 5 nN (grey).

behaviour between the left and the right edge of the features. At the left edge friction force is enhanced, while at the right edge not even a topographic effect is visible within the experimental resolution of about 4 nN.

Besides the described phenomena no variation in the friction behaviour is observable. This is not surprising, since the sample, immersed in electrolyte after cleavage, is chemically homogeneous. Thus the friction coefficient should stay constant on the entire surface [15].

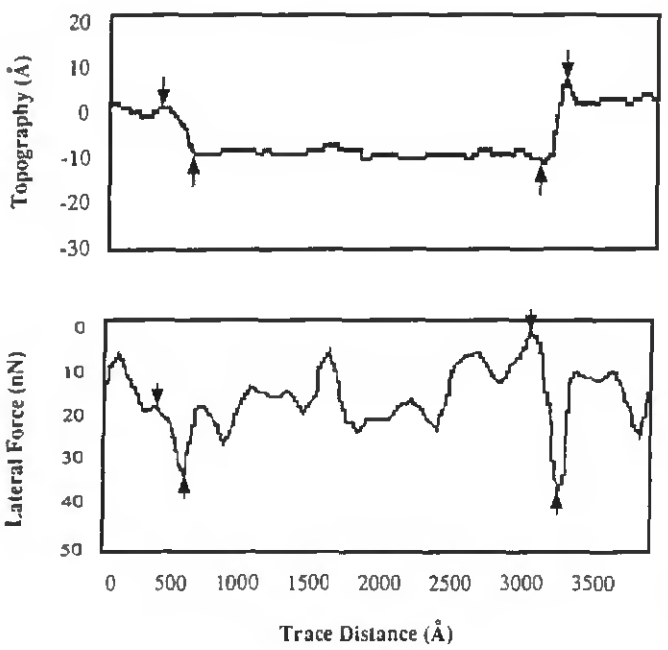

Figure 3. Section through both the topographic (upper trace) and the friction force data (lower trace), corresponding to the black line in figure 2 lower left. The two curves evidence the effect of step edges (marked with corresponding arrows) on the friction force behaviour. For discussion see text.

Figure 4 shows a topographic image of the sample area marked with a rectangle on figure 2, containing a series of force/distance curves. Curves 1, 2 and 4 show the expected behavour of a rigid surface, with a snapping of the cantilever on approaching, due to attractive forces present even in the electrolytic environment. The hysteresis of the curves is caused by the weak spring constant of the cantilever. Most interestingly, curve 3, taken on the large, three-atom-high tongue-shaped terrace just beside a monoatomic step, does not show this typical behaviour, but is of a symmetric, almost continuous form instead of showing a sharp cusp.

The assumption of a loosely bound graphite terrace might account for the strange shape of curve 3. From this curve we calculate an effective spring constant of the tongue of 0.05 N m^{-1}. This value can be compared to an estimated spring constant for a cantilevered graphite flake of 1.2 nm height and of 100 nm width and length. Assuming that the Young's modulus for the flake is the same as for bulk graphite, we obtain a spring constant of $k \cong 10^{-3}$ N m^{-1}.

The agreement in the order of magnitude between the measured and estimated values and the shape of the terrace suggest that the assumption of a cantilevered flake might be correct.

To our knowledge a feature like this has never been imaged before. Most probably in conventional SFM measurements in air or UHV, the applied loads due to attractive van der Waals forces are far too high for imaging unstable structures like these and they are just wiped away.

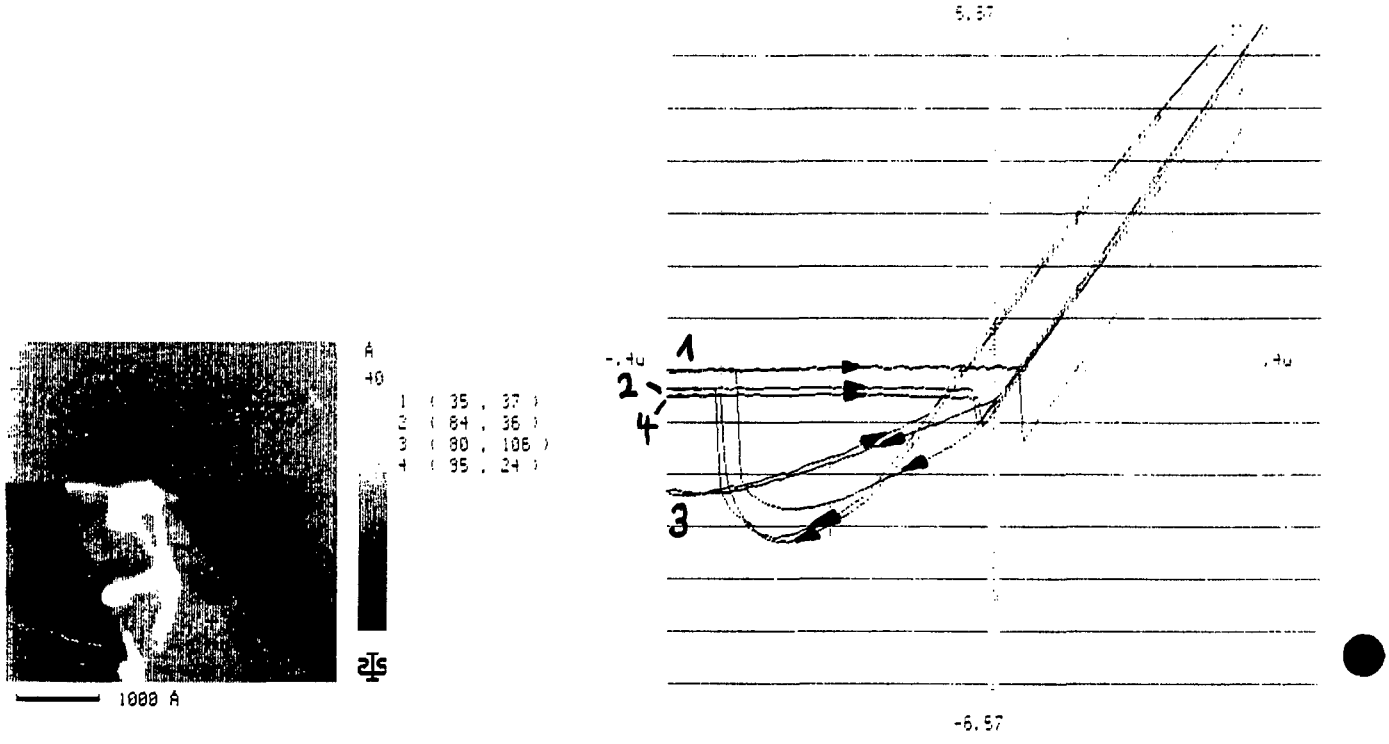

Figure 4. Series of force/distance curves on the uppermost part of the large tongue in figure 2 (small topographic image corresponding to the rectangle). Note the particular appearance of curve 3. Curves were recorded above the sample spots marked with corresponding crosses on the topographic image. Further explanations in text.

4. Conclusions and outlook

It was possible to show the principal feasibility of measuring simultaneously normal (load) and lateral (friction) forces in an *in situ* SFFM experiment in an electrolytic environment under potentiostatic control of the sample. Although initial results are not completely understood and certainly need to be complemented with further experiments, they are considered as very promising in terms of opening an enormous field of interesting applications.

Not only thermodynamically unstable samples or adsorbates can be studied under potential control with potentiostatic SFFM, but also soft or delicate ones, because of the reduced load due to the aqueous environment [20, 21] as could be shown on the loosely adhered flakes of the test sample. Providing absolute calibration facility, the SFFM also permits investigation of the shear strength of adsorbed species [15], which allows one to obtain a more profound knowledge of the thermodynamics and kinetics of chemical and/or physical adsorption processes.

A further fascinating field for quantitative atomic/molecular friction studies is the investigation of the Helmholtz double layer, which is not yet perfectly understood.

Furthermore the potentiostatic SFFM opens new ways to investigate technically relevant tribosystems under well defined, nevertheless realistic, conditions down to atomic scale. Together with fundamental adhesion and friction studies [15, 22] under different conditions and in combination with molecular dynamics calculations [23, 24], this approach will eventually lead to a better understanding of macroscopic tribomechanisms.

One of the most exciting features of the SFFM is its ability to distinguish different materials due to changes in the friction coefficient, which the inventors called 'chemical sensitivity' [15, 25, 26]. Thus, the method also promises great potential in general chemical/electrochemical analysis, covering important aspects in fields such as corrosion, catalysis and photochemistry.

Acknowledgments

The authors would like to thank R Nyffenegger and J Béguin for generous cooperation, the Swiss National Foundation for Scientific Research and the Deutsche Forschungsgesellschaft for supporting the work (NFP 24 and SFB 306), and finally U Duerig, H Rohrer and A Savan for helpful discussions.

References

[1] See, e.g.
Dowson D 1979 *History of Tribology* (London: Longman)
Johnson K L 1985 *Contact Mechanics* (Cambridge: Cambridge University Press) and references therein
[2] Binnig G, Rohrer H, Gerber Ch and Weibel E 1983 *Phys. Rev. Lett.* **50** 120
[3] Binnig G, Quate C F and Gerber Ch 1986 *Phys. Rev. Lett.* **56** 930
[4] Mate C M, McClelland G M, Erlandsson R and Chiang S 1987 *Phys. Rev. Lett.* **59** 1942

[5] Marti O, Colchero J and Mlynek J 1990 *Nanotechnology* **1** 141
[6] Meyer G and Amer N M 1990 *Appl. Phys. Lett.* **56** 2100
[7] Sonnenfeld R and Hansma P K 1986 *Science* **232** 221
[8] Marti O, Drake B and Hansma P K 1987 *Appl. Phys. Lett.* **51** 484
[9] Lustenberger P, Rohrer H, Christoph R and Siegenthaler H 1988 *J. Electroanal. Chem.* **243** 225
[10] Lev O, Fan F-R and Bard A J 1988 *J. Electrochem. Soc.* **135** 783
[11] Binggeli M, Carnal D, Nyffenegger R, Siegenthaler H, Christoph R and Rohrer H 1991 *J. Vac. Sci. Technol.* B **9** 4, 1985
[12] Siegenthaler H 1992 *STM in Electrochemisty (Springer Series in Surface Science vol 28)* ed H-J Güntherodt and R Wiesendanger (Berlin: Springer) and references therein
[13] Manne S, Hansma P K, Massio J, Elings V B and Gewirth A A 1991 *Science* **251** 183
[14] Hipp M, Bielefeldt H, Colchero J, Marti O and Mlynek J 1992 *Proc. 6th Int. Conf. on STM (Interlaken), Ultramicroscopy* **42-44**
[15] Marti O, Colchero J and Mlynek J 1992 *NATO-ARW on Manipulation of Atoms under High Fields (Lyon, 1992)* (Deventer: Kluwer) to be published
[16] Park Scientific Instruments
[17] Prototype kindly provided by R Nyffenegger, University of Berne/Park SI
[18] Union Carbide, L4470, graphite monochromator ZYB
[19] Merck p.a.
[20] Garcia N and Goodman F O 1992 *Proc. 6th Int. Conf. on STM (Interlaken), Ultramicroscopy* **42-44**
[21] Ciraci S 1992 *Proc. 6th Int. Conf. on STM (Interlaken), Ultramicroscopy* **42-44**
[22] Dürig U and Züger O *NATO-ARW on Manipulation of Atoms under High Fields (Lyon, 1992)* (Deventer: Kluwer) to be published
[23] Landman U, Luedtke W D and Ringer E M 1992 *Wear* **153** 3
[24] Joaquin Ch. *NATO-ARW on Manipulation of Atoms under High Fields (Lyon, 1992)* (Deventer: Kluwer) to be published
[25] Colchero J, Bielefeldt H, Ryf A, Hipp M, Marti O and Mlynek J 1992 *Phys. Status Solidi* a **131** 73
[26] Meyer E, Overney R and Frommer J to be published

Novel design for a compact fiber-optic scanning force microscope

M. Binggeli, G. Kotrotsios, R. Christoph, and H. E. Hintermann
Centre Suisse d'Electronique et de Microtechnique, Rue Breguet 2, CH-2007 Neuchâtel, Switzerland

Th. Berghaus and P. Güthner
Omicron Vakuumphysik GmbH, Idsteinerstrasse 78, D-6204 Taunusstein 4, Germany

(Received 14 July 1992; accepted for publication 2 July 1993)

We present a new scanning force microscope (SFM) design with a compact fiber-optic interferometric detection system that provides very high resolution for surface force measurements. The mechanical conception of the instrument includes the implementation of piezoelectric actuators for the interferometer alignment. The result of this approach is a high performance SFM with both easy handling and high versatility.

I. INTRODUCTION

Scanning force microscopy (SFM)[1] is a new and very powerful surface analytical technique which is now used worldwide by an impressive number of surface and interface scientists.[2] Force microscopes probe the sample under investigation with a cantilever stylus that converts a local surface force into a measurable displacement. SFM permits investigation of a vast variety of conducting and nonconducting samples with up to atomic resolution in both liquid or gaseous environments.

The continuous proliferation of new SFM techniques such as noncontact imaging[3] and bidirectional SFM[4] implies a growing need for new instrumentation. This instrumentation should not only be of high performance with respect to resolution, handling, and reliability but also cover the widest possible range of SFM applications, including SFM studies in electrochemistry, tribology, magnetism, photography, and biology. In order to meet this demand on instrumental versatility, we have chosen a design using a fiber-optic interferometer combined with piezoelectric actuators for force sensing, which permits both easy direct access to all experimental parameters and the implementation of new measurement techniques.

II. SFM DESIGN

The microscope is integrated on a solid ground plate and is basically built of two main units:

(1) *The measuring head,* which contains the force sensor and three micrometer screws for the positioning of the sensor on the axis perpendicular to the sample surface;

(2) *The base,* which consists of a 30-mm solid Al ground plate containing a high-precision x/y stage and a housing for the interferometric setup. The x/y stage is used for the lateral coarse positioning of the force sensor versus sample and exhibits an opening at its center providing space for a piezoelectric tube scanner with sample holder, mounted directly to the x/y table. For easy sample exchange the samples are magnetically clamped to the sample holder. A schematic representation of the measuring head containing the motors and the force sensor, placed on the x/y stage is depicted in Fig. 1.

The measuring head is manually removable, in order to facilitate the renewal of the force sensor and for sample exchange. For operation, the head is set on top of the x/y stage with the ends of the three micrometer screws forming a stable tripod, which is an improved version of a system that has proven its capability before.[5,6] In this configuration, the force sensor is located above the center of the sample holder and can be laterally moved over the sample with the x/y stage.

A. Force sensor

The central part of the presented force microscope is its force sensor. It consists of a cantilever beam (all common types) that probes the surface. The deflections of the cantilever beam are measured with a fiber-optic interferometer demonstrated by Rugar *et al.*[7,8] and also described by other authors.[9] This detector system uses a pigtailed laser diode directly spliced to a 2×2 fiber coupler. Especially, this feature allows for a very compact instrument layout, thus enhancing the stability of the SFM. The adjustment of the relative position of the fiber end of the interferometer and the cantilever is performed with two independent piezodriven inertial stepper motors. In each of these two motors, a hardened steel slider sits on three aluminum oxide balls (special materials were chosen in order to avoid friction losses during operation), each one being

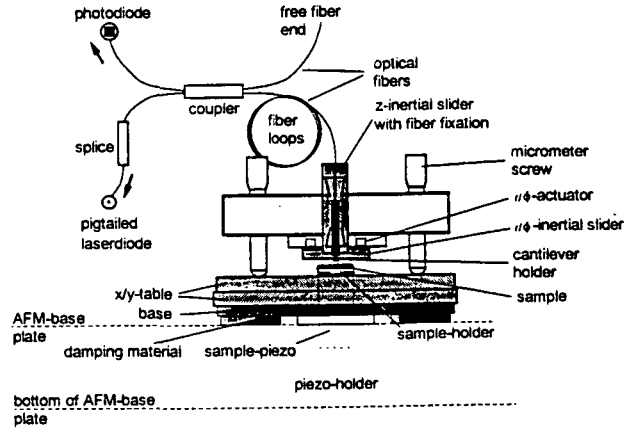

FIG. 1. Schematic representation of the microscope showing the measuring head (a third screw located at the back is hidden by the force detector) set on top of a precision x/y table. The arrangement of the two independently driven motors for the z and r/Φ inertial slider as well as the optical detection system are shown.

 0034-6748/93/64(10)/2888/4/$6.00

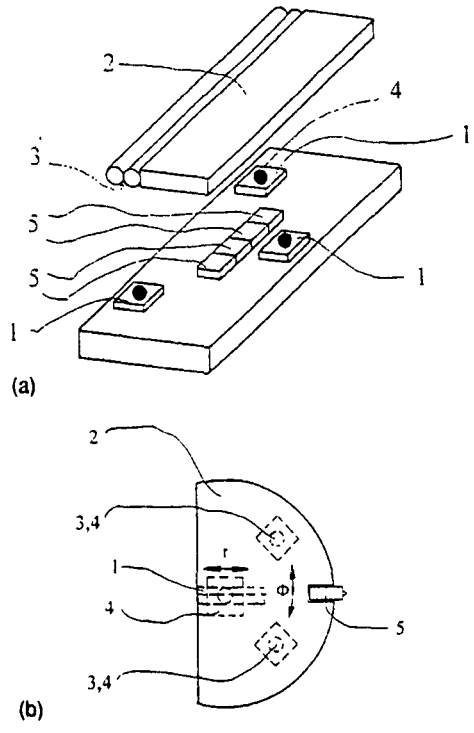

FIG. 2. (a) Perspective view of the motor performing the approach between fiber end and cantilever: (1) shear piezos, (2) slider, (3) V groove, (4) ceramic balls, (5) magnets. (b) r-Φ inertial slider for positioning the slider with respect to the fiber: (1) r axis V groove, (2) slider, (3) ceramic balls for Φ motion, (4) ceramic balls for r motion, (5) cantilever.

mounted on a shear piezo stack. In order to hold this slider on its support a normal force is applied on the slider by magnets, mounted between the shear piezo stacks. The magnetic principle has the advantage that the motor's operation is independent of its orientation. For a single-step operation, a slowly increasing voltage is first applied to the piezoelectric transducer. This produces a corresponding slow shear displacement of the transducer until it reaches its maximum value. In this phase, the slider follows the transducer movement. In a second phase, the voltage is rapidly decreased from its maximum to its initial value. This results in a correspondingly fast return of the piezoelectric transducer to its initial position. In this latter case however, the slider will remain at its position due to mass inertia.[10] The step size depends on the magnitude of the voltage pulse. According to the quality of the slider surface, experience shows that the smallest reproducible step size is approximately 20 nm. The maximum achievable step size with the control unit used in our experiments is 400 nm. These steps can be performed in rapid sequences, thus enabling movements of the order of millimeters within a few seconds.

The SFM described comprises two different independently driven motors. A first motor is used to adjust the spacing between fiber end and cantilever [Fig. 2(a)]. This operation requires a linearly guided movement of the slider, which is achieved by a special slider/support configuration. The slider consists of a rectangular metal piece as shown schematically in Fig. 2(a). The side of the slider adjacent to the support possesses a V groove along its length axis. The slider rests on the support with two of the three ceramic balls being located in this V groove, thus guiding the slider's movement.

A second motor is used for the lateral positioning of the slider with respect to the fiber end. This operation requires two different axes of slider motion, marked as "r" and "Φ" in Fig. 2(b). The slider is shaped as a circle segment which exhibits a V groove in the central part backside. As shown schematically in Fig. 2(b) the piezo actuators are configured in such way that they can perform a movement parallel to the r axis (valid for all three elements) and perpendicular to this direction [valid only for the two actuators marked as Φ in Fig. 2(b)]. The ceramic ball located in the groove acts either as a guide for the slider motion along the r direction or as a pivot for the circular motion of the cantilever which results when the Φ actuators are driven.

B. Operation

The measuring configuration is obtained as follows: First, the lateral position of cantilever versus fiber is adjusted in order to obtain a maximum of reflected light off the surface at the cantilever apex. The fiber is then approached to the cantilever to a distance of a few microns. Figure 3 shows an example of the interferometric response when the fiber is stepped towards the cantilever over a

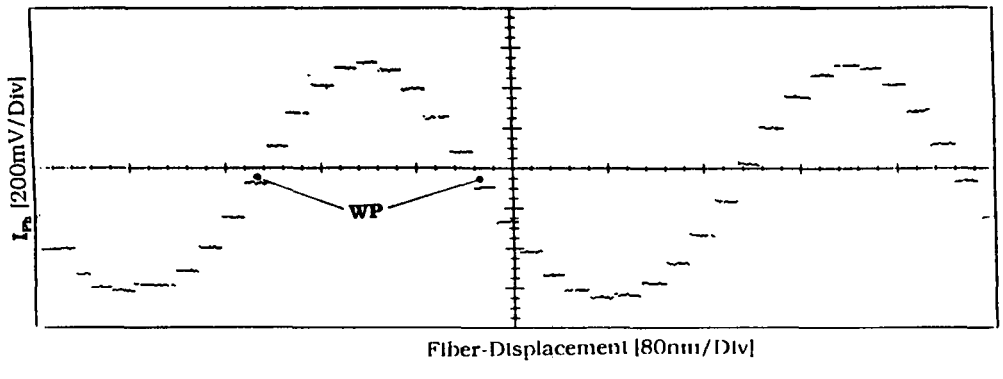

FIG. 3. Oscilloscope plot of the photocurrent response to a series of steps with the fiber end towards the cantilever. WP (working point) corresponds to the midpoint current.

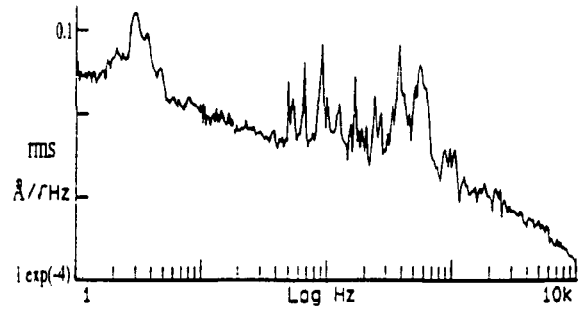

FIG. 4. Noise-density spectrum of the instrument. I_{ph} was measured with the cantilever touching the surface but without scanning the sample.

distance of about 800 nm. The fringe visibility V, given by $V=(i_{max}-i_{min})/(i_{max}+i_{min})$, typically shows values of 0.8–0.9. The fiber is left at the midpoint current, a spacing corresponding to an intensity gradient maximum of the sinusoidal interference pattern (referred to as "working point" WP in Fig. 3). This configuration, chosen in order to get maximum sensitivity, is very stable and allows even to repeatedly take the measuring head off its stage (i.e., to exchange the sample) without altering the interferometer adjustment.

The approach of the force sensor towards the sample is executed mechanically with the three precision micrometer screws integrated in the head. The coarse approach is performed with the two front screws (shown in Fig. 1), the fine approach with the third one in the back (1:8 movement reduction with respect to coarse approach). When tip and sample are in mechanical contact, the current intensity at WP is used as set point value for the feedback loop of the control unit. The tip/sample interaction force is regulated by stepping the fiber forward/backward while keeping a constant fiber/cantilever spacing with the control loop acting on the substrate piezo.

In this final configuration the instrument is ready for imaging, which is performed by scanning sample versus tip and simultaneously recording the feedback response.

III. EXPERIMENTAL RESULTS

First measurements proved the instrument's stability. Figure 4 shows a noise-density spectrum achieved by measuring the unfiltered interferometric response from the photodiode (I_{ph}) in ambient air. This measurement was performed with the cantilever being in contact with the sample in order to show the stability of the entire instrument. No special precautions were taken with respect to damping mechanical and acoustical vibrations but placing the instrument on an air-damped antivibration table. The peak at ~4 Hz corresponds to the lowest resonance of the table, those around 800 Hz are due to the resonances of its stony top slab. The noise floor at 1 kHz is $2E$-3 Å/$\sqrt{\text{Hz}}$. Typically, the integrated rms noise in a bandwidth of 10 kHz is smaller than 0.5 Å. Care should be taken when comparing these results with other work (e.g., Refs. 11 and 12), since they generally describe the stability of displacement sensors on a free cantilever. The signal/noise ratio can still be improved substantially by, for example, isolating the laser diode, controlling its temperature, and undertaking further efforts on the acoustic isolation of the microscope.

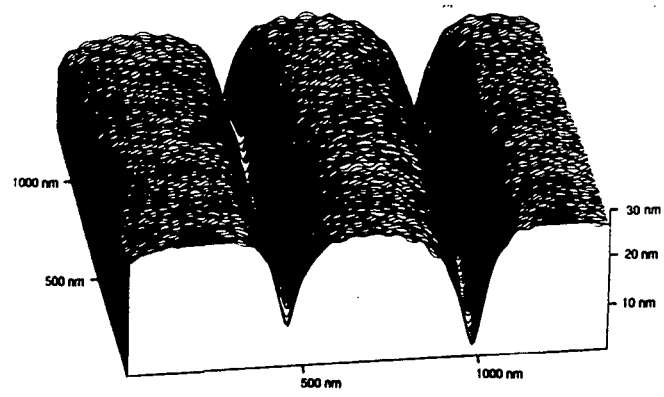

FIG. 5. Grey scale image of a 1.5×1.5 μm^2 area of an optical grating manufactured by CSEM.

Figure 5 shows an example of an image measured with the instrument using Omicron control electronics and software. This line plot represents a 1.5×1.5 μm^2 area of grating etched in glass as used for guided wave optic devices. The presented results show the performance of an instrument unifying a series of advantageous features, which include the following:

(i) Very high resolution in air, due to the extremely short optical path length of the displacement sensor,

(ii) Easy-to-handle implementation of the fiber-optic interferometer principle due to the fiber/cantilever adjustment facility described in paragraph II. It allows a straightforward setup of the interferometer since there are only two components to align.

(iii) Possibility of a direct interferometric calibration of the z axis of the scanner simply using a mirror-like substrate.

(iv) Easy access to a direct calibration of x and y axis by mounting a little mirror on the side of the piezo and approaching the fiber with the x/y stage.

(v) Precise (micron-range) orthogonal preadjustment of the sample area to be investigated with the x/y stage.

(vi) Access to ac mode technique in order to perform noncontact SFM, with a wide range of new applications as, e.g., probing of electrostatic or magnetic properties of the sample, imaging of biological samples, etc.

As a consequence of the mentioned characteristics this SFM constitutes a device that leaves an outstanding degree of freedom to the experimentalist carrying out his experiments. Interesting applications could also emerge in industrial quality control, due to the instrument's precise and strictly orthogonal detector position control and its rigidity resulting from the application of the pigtail technique.

ACKNOWLEDGMENTS

The authors would like to thank R. Höhener for computer assistance, S. Droz for technical advising, P. Sixt for

providing the optical grating, J. Burger for helpful discussions, and finally Omicron Vakuumphysik GmbH for financially supporting the development.

[1] G. Binnig, C. F. Quate, and Ch. Gerber, Phys. Rev. Lett. **56**, 930 (1986).
[2] Proceedings of STM conferences in Baltimore 1990 [J. Vac. Sci. Technol. B 9, 2(II) (1991) and Interlaken 1991, Ultramicroscopy **42–44**, (1992)].
[3] U. Dürig, J. K. Gimzewski, and D. W. Pohl, Phys. Rev. Lett. **57**, 2403 (1986).
[4] O. Marti, J. Colchero, and J. Mlynek, Nanotechnol. **1**, 141 (1990).
[5] M. Binggeli, D. Carnal, R. Nyffenegger, H. Siegenthaler, R. Christoph, and H. Rohrer, J. Vac. Sci. Technol. B 9, 1985 (1991).
[6] R. Christoph, H. Siegenthaler, H. Rohrer, and H. Wiese, Electrochim. Acta **34**, 1011 (1989).
[7] D. Rugar, H. J. Mamin, R. Erlandsson, J. E. Stern, and B. D. Terris, Rev. Sci. Instrum. **59**, 2337 (1988).
[8] D. Rugar, H. Mamin, and P. Guethner,Appl. Phys. Lett. **55**, 2588 (1989).
[9] S. Mulhern, T. Hubbard, C. S. Arnold, B. L. Blackford, and M. H. Jericho, Rev. Sci. Instrum. **62**, 1280 (1991).
[10] Deutsche Patentschrift DE 4023311 C2 (17 December 92).
[11] Ch. Schönenberger and S. F. Alvarado, Rev. Sci. Instrum. **60**, 3131 (1989).
[12] D. Anselmetti, Ch. Gerber, B. Michel, H.-J. Güntherodt, and H. Rohrer, Rev. Sci. Instrum. **63**, 3003 (1992).

Influence of capillary condensation of water on nanotribology studied by force microscopy

M. Binggeli
Centre Suisse D'Electronique et de Microtechnique (CSEM), CH-2007 Neuchatel, Switzerland

C. M. Mate
IBM Research Division, Almaden Research Center, San Jose, California 95120

(Received 24 March 1994; accepted for publication 9 May 1994)

The influence of capillary condensation and humidity to friction and adhesion properties on a nanometer scale has been studied using a bidirectional force microscope. On a hydrophilic silicon oxide surface strong capillary formation could be observed at high humidities, whereas, on less hydrophilic amorphous carbon films and lubricated silicon oxide surfaces, capillary formation is suppressed. The hydrophilicity of the surface is also found to promote the lubricative effects of adsorbed water.

Most surfaces under normal conditions are covered by thin layers of molecules directly absorbed from their environment. Because of its abundance and particular chemical properties, water is one of the more important adsorbant molecules. Even adsorbed water films of only a few molecules in thickness can dramatically influence the corrosion and wear properties of surfaces (e.g., Ref. 1). In order to simulate the effect of capillary condensation of water around contacting surfaces on nanoscale friction and adhesion, we have studied the condensation of water around a sharp point, the tip of an atomic force microscope (AFM), in contact with a flat surface. The ability of AFM to measure the minute forces acting on the tip makes it a unique instrument for studying the nanoscale tribology of single asperity contacts, as demonstrated in several previous AFM tribology studies.[2–7] Two types of experiment are conducted: normal force versus tip-sample separation distance (dipping) and friction versus load during scanning. We find very little effect for relative humidities less than 75%, but, as the humidity approaches saturation, substantial water capillaries condense around the tip and strongly affect the nanotribological behavior. The hydrophilicity of the surface is found to favor the formation of the water capillary and the lubricative effect on the adsorbed water.

The force microscope used for these experiments is shown schematically in Fig. 1. The microscope is similar to some described previously[6,8] and uses two optical fibers for independently measuring the friction and load components of the force acting on the tip. The force microscope cantilevers, with spring constants 30–70 N/m, are obtained by bending 50 μm diam tungsten wires at a right angle and etching the ends to a sharp tip, typically 1000 Å in radius. For environmental control, the force microscope was placed into a closed box with inlets for dry and H_2O saturated nitrogen.

Samples studied were chosen to be relevant to disk drive technology where humidity is known to have a major effect on the durability and friction forces experienced at the recording head/disk interface.[9,10] The samples were silicon (100) wafers covered (1) with clean native silicon oxide (~12 Å thick), (2) with a 250 Å thick amorphous carbon film, and (3) with 15 Å thick perfluoropolyether lubricant (Fomblin Z-Dol), which was thermally bonded to the silicon oxide.[5,6] The contact angles of water on these surfaces were 2° for clean silicon oxide, 45° for amorphous carbon, and 80°–90° for the perfluoropolyether lubricant.

The dipping experiments (normal force versus separation distance) are used to monitor the growth of the water film on sample and tip and the growth of the water capillary around the tip during contact as a function of relative humidity. The inset in Fig. 2 shows the force versus distance curves for two extremes of relative humidity, near 0% and at 97%, as an amorphous carbon sample is brought into contact with the tip and then withdrawn. The tip first experiences an attractive force on approach at point A, which is interpreted as the onset of capillary condensation. At near 0% relative humidity, the capillary condensation presumably originates from contaminants,[5] such as hydrocarbons and small amounts of water. As the sample further approaches the tip, the normal force eventually turns repulsive and, at point B, goes through zero force. As the sample is withdrawn, after breaking the solid-solid adhesion (minimum force in curve), the attractive force from the capillary meniscus gradually decreases to point C. The distance from B to C, called the break-free length[11] is a measure of the size of the capillary meniscus that forms around the tip and sample during contact. Figure 2 shows a plot of break-free lengths on the three investigated samples as a function of relative humidity. The positive off-

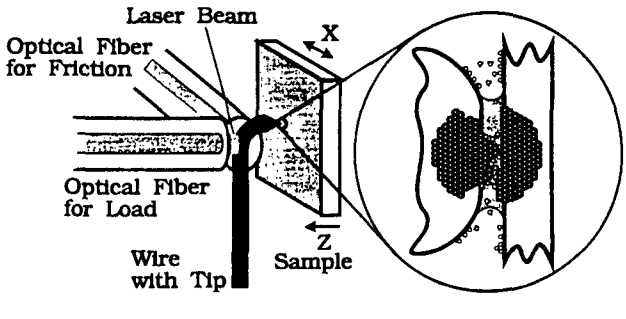

FIG. 1. Schematic representation of the bidirectional force microscope, with tip, sample, and the two optical fibers. The zoom shows the tip-sample contact region with the water meniscus and molecules.

 0003-6951/94/65(4)/415/3/$6.00

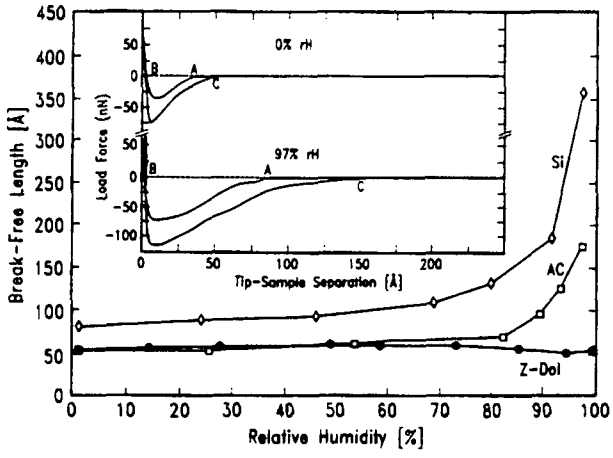

FIG. 2. Break-free length (distance B-C on inset) as a function of relative humidity for the clean Si(100) wafer (Si), the amorphous carbon film (a-C), and the bonded perfluoropolyether film (Z-Dol). The inset depicts two dipping experiments on amorphous carbon, at 0% and 97% relative humidity (rH).

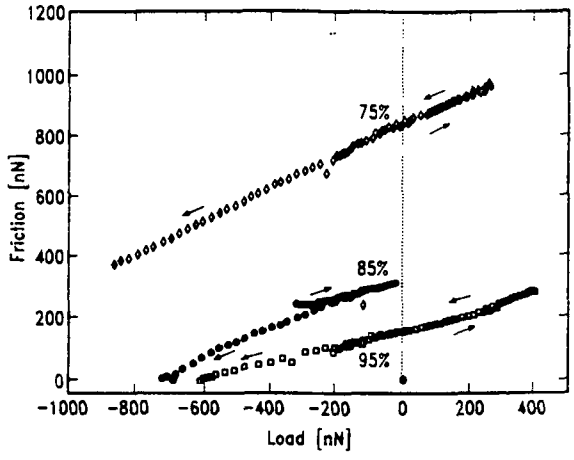

FIG. 3. Friction vs load at different humidities on a silicon oxide surface on a Si(100) wafer. The arrows indicate whether the load is increasing or decreasing.

set at low humidities originates from surface contaminants as mentioned above. For the hydrophilic silicon oxide surface, the break-free length, and hence the size of the meniscus, grows dramatically as the relative humidity approaches saturation, as should be expected from the Kelvin equation.[12] On the lower energy, or more hydrophobic surfaces of amorphous carbon and lubricated silicon, less contaminants are present at low humidities and water capillary formation is quenched at high humidities. These results are consistent with those of Pashley and Kitchener,[13] who observed that the thickness of the adsorbed water film on quartz surfaces was sensitive to surface cleanliness and preparation.

The friction studies were carried out as follows: the sample is scanned back and forth in the x direction, while the load is first increased then decreased. Sliding speeds were on the order of μm/s. At low to moderate humidities (<75%), no special effects are observed, besides a "wearing in" of the tip, causing an increase in adhesive force. For high relative humidities (>75%), the influence of adsorbed water was readily apparent. Figure 3 shows some of the friction experiments at high humidities for a clean silicon wafer. Each data point represents the average friction and load during sliding over one cycle x. Even at these ultralow loads, friction is observed to be linear with load, implying that the actual contact occurs through mutiple asperity contacts,[14] as illustrated in Fig. 1. The slopes of the linear friction versus load curves provide the friction coefficients μ and extrapolating the curves to zero friction force yields an estimate of the adhesive forces during sliding. The strong dependence of the friction properties on the humidity is clearly apparent: μ drops from 0.5 to 0.25 and the adhesive force drops from 1.5 to 0.7 μN. Figure 4 compares the behavior of the friction coefficient [Fig. 4(a)] and the adhesive forces [Fig. 4(b)] as a function of relative humidity for silicon and amorphous carbon.

We understand the decrease in adhesive force during sliding with increasing humidity as a superposition of physical and chemical phenomena. For boundary lubricated systems, most of the load is supported by the lubricant film surrounding the contacting asperities,[15] in our case water from capillary condensation. The adhesive force on the tip is the sum of the capillary force and the interaction force between the two solid surfaces mediated by the water in the gaps between the contacting asperities. For a spherically shaped tip in contact with a flat surface at high humidities, the capillary force is independent of humidity and well approximated[12] by $F_{cap} \simeq 4\pi R\gamma \cos\theta$, where R is the tip radius, γ the surface tension of water, and θ the contact angle of water on the surfaces. The solid-solid interaction is more complicated than the capillary force. It can consist of van der Waals forces, electrostatic forces, and chemical bonding. The presence of water in the gap can greatly change the nature of the interaction. Since the liquid water is at equilibrium with the water vapor, the chemical potential of the liquid in the gaps around the contacting asperities is

$$\mu_1 = kT \ln(p/p_s). \tag{1}$$

From thermodynamics, the component of the attractive force acting on the tip from the liquid in the gaps is given by

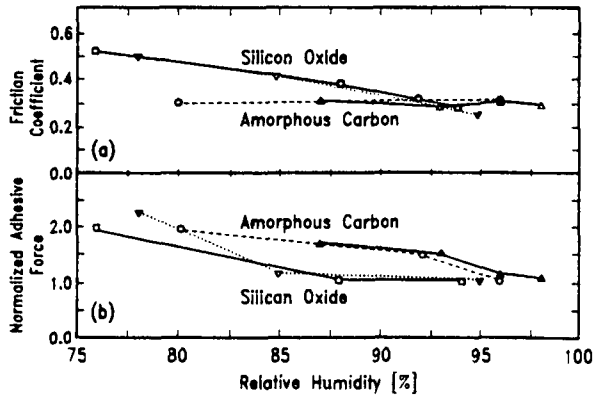

FIG. 4. Friction coefficients and normalized adhesive forces during sliding as a function of relative humidity. Two typical measurements series for clean silicon wafers with silicon oxide and amorphous carbon are shown. Adhesive forces have been normalized by setting the lowest value to 1 to account for different tip radii in the separate experiments.

$$F = -\frac{\partial G}{\partial z} = -\frac{A}{v}\mu_l = -\frac{A}{v}kT\ln\left(\frac{p}{p_s}\right), \quad (2)$$

where G is the Gibb's free energy, A the area of the liquid film, and v the molar volume. Therefore, the force from water in the gaps becomes less attractive, i.e., more repulsive, with higher relative humidity, consistent with the reduction in adhesive forces observed in the friction experiments at higher humidities. For the carbon films, the decrease in adhesive force occurs at higher humidities [Fig. 4(b)] than for silicon oxide, most likely due to the lower wettability of these films, reflected by the larger contact angle and the suppressed capillary formation (Fig. 2).

Figure 4(a) shows that the friction coefficient decreases with increasing humidity for silicon oxide but not for carbon. From the decrease in the friction coefficient on silicon oxide, we infer that, as the water partial pressure increases, unbound water molecules are pushed into the microasperity contact junctions, reducing the shearing force necessary to move the two surfaces past each other. On amorphous carbon, however, the water molecules apparently are unable to penetrate the contact junctions. The difference between silicon oxide and carbon can be explained by the more hydrophilic nature of the oxide, where water molecules are strongly bound to the surface by hydrogen bonding to the abundant hydroxyl groups.[16,17] The friction measurements carried out on lubricant covered silicon oxide showed a complex mix of the above discussed effects, which shall be described in a future publication.

In conclusion, the forces acting on an AFM tip in contact with silicon and carbon surfaces have been studied as a function of relative humidity to help understand the effect of adsorbed water vapor in tribology. On a hydrophilic surface, large capillaries form at relative humidities above 70% and adhesive forces and friction coefficients decrease substantially for a sliding AFM tip. On a more hydrophobic surface, capillary condensation of water is greatly reduced and a decrease is observed only in adhesive forces.

We would like to thank Dr. G. I. Rudd, Dr. A. Homola, Dr. G. M. McClelland, and Dr. S. S. Perry for helpful discussions, R. L. White for preparation of the amorphous carbon films, and especially Professor H.-E. Hintermann, recipient of the 1992 Forum Engelberg Award, who designated the scholarship as part of the award to M. Binggeli to carry out this study at IBM Almaden and who initiated and inspired the work on this subject. M. Binggeli would also like to thank IBM Switzerland and CSEM for financial support during this joint study.

[1] P. Niederhaeuser, H.-E. Hintermann, and M. Maillat, Thin Solid Films **108**, 119 (1983).
[2] C. M. Mate, G. M. McClelland, R. Erlandsson, and S. Chiang, Phys. Rev. Lett. **59**, 1942 (1987).
[3] O. Marti, J. Colchero, and J. Mlynek, Nanotechnology **1**, 141 (1990).
[4] N. A. Burnham, D. D. Dominguez, R. L. Mowery, and R. J. Colton, Phys. Rev. Lett. **64**, 1931 (1990).
[5] G. S. Blackman, C. M. Mate, and M. R. Philpott, Phys. Rev. Lett. **65**, 2270 (1990).
[6] C. M. Mate, Phys. Rev. Lett. **68**, 3323 (1992).
[7] E. Meyer, R. Overney, D. Brodbeck, L. Howald, R. Luthi, J. Frommer, and H.-J. Guntherodt, Phys. Rev. Lett. **69**, 1777 (1992).
[8] D. Rugar, H. J. Mamin, and P. Guethner, Appl. Phys. Lett. **55**, 2588 (1989).
[9] R. S. Timsit and G. Stratford, Tribol. Mech. Magn. Storage Syst. **5**, 17 (1988).
[10] A. M. Homola, Adv. Info. Storage Syst. **1**, 279 (1991).
[11] C. M. Mate and V. J. Novotny, J. Chem. Phys. **94**, 8420 (1991).
[12] J. N. Israelachvili, *Intermolecular and Surface Forces: With Applications to Colloidal and Biological Systems* (Academic, New York, 1985), p. 223.
[13] R. M. Pashley and J. A. Kitchener, J. Colloid Interface Sci. **71**, 491 (1978).
[14] J. A. Greenwood and J. B. P. Williamson, Proc. R. Soc. Lond. A **295**, 300 (1966).
[15] A. W. Adamson, *Physical Chemistry of Surfaces* (Wiley, New York, 1990), p. 479.
[16] A. W. Adamson, *Physical Chemistry of Surfaces* (Wiley, New York, 1990), p. 279.
[17] J. N. Israelachvili, *Intermolecular and Surface Forms: With Applications to Colloidal and Biological Systems* (Academic, New York, 1985).